ORGANOMETALLICS

pubs.acs.org/Organometallics

Article

Low-Valent Molybdenum PNP Pincer Complexes as Catalysts for the Semihydrogenation of Alkynes

Niklas F. Both, Anke Spannenberg, Kathrin Junge,* and Matthias Beller*

Cite This: *Organometallics* 2022, 41, 1797−1805

Read Online

ACCESS | Metrics & More | Article Recommendations | Supporting Information

ABSTRACT: Low-valent molybdenum PNP pincer complexes were studied as catalysts for the semihydrogenation of alkynes. For that purpose, *t*Bu-substituted PNP complexes PNP^{tBu}Mo(CO)$_2$ (**6a**) and PNP^{tBu}Mo(CO)$_3$ (**6c**) and the NNP complex NNP^{iPr}Mo(CO)$_2$(PPh$_3$) ((*rac*)-**7**) were synthesized and characterized. By utilizing the cyclohexyl-substituted complex PNP^{Cy}Mo(CO)$_2$(CH$_3$CN) (**5a**), several diphenylacetylene derivatives are transformed to the corresponding (*Z*)-alkenes with good to very good diastereoselectivities (up to 91:9). Mechanistic experiments indicate an outer-sphere mechanism including metal−ligand cooperativity.

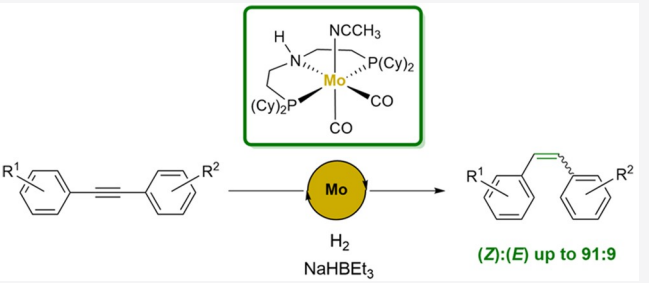

INTRODUCTION

The conversion of alkynes to alkenes plays an important role in the bulk and fine chemical industry as well as in basic chemical research.[1,2] Although numerous methods for the synthesis of alkenes have been developed in the past, the catalytic semihydrogenation of alkynes with dihydrogen is arguably one of the most efficient and atom economic approaches in this respect. However, it continues to be challenging due to the required control of stereo- ((*Z*)/(*E*)-isomers) and chemoselectivity (alkynes vs alkenes).

Typically, in this transformation heterogeneous systems based on noble metals, in particular Pd,[3,4] are utilized such as the well-known Lindlar's catalyst (Pb-poisoned Pd/CaCO$_3$).[5] With growing importance of sustainability and resource scarcity, over the past decade many efforts were made to develop catalysts derived from more available and cheaper non-noble metals, especially from the first-row transition metals.[6] More specifically, both heterogeneous and homogeneous systems based on Cr,[7] Fe,[8−11] Mn,[12,13] Co,[14−16] Ni,[17−19] and Cu[20] have been studied for this transformation.

For homogeneous, non-noble metal systems, the first report dates back to 1989, when Bianchini and co-workers discovered that iron(II) complex **I** with a tetradentate phosphine ligand is capable of selectively hydrogenating terminal alkynes to the corresponding alkenes (Figure 1).[8,9] In 2013, the group of Milstein described acridine-based PNP iron(II) pincer complex **II** with an amidoborane coligand for the (*E*)-selective semihydrogenation of alkynes.[10] Initially, in this process the (*Z*)-alkene is formed which is rapidly isomerized to its (*E*)-isomer. Later, Fout and co-workers reported cobalt(I) dihydrogen complex **III** bearing a CCC pincer ligand with two NHC moieties for the (*E*)-selective semihydrogenation of a broad scope of alkynes.[14] As in the case of iron complex **II**, the

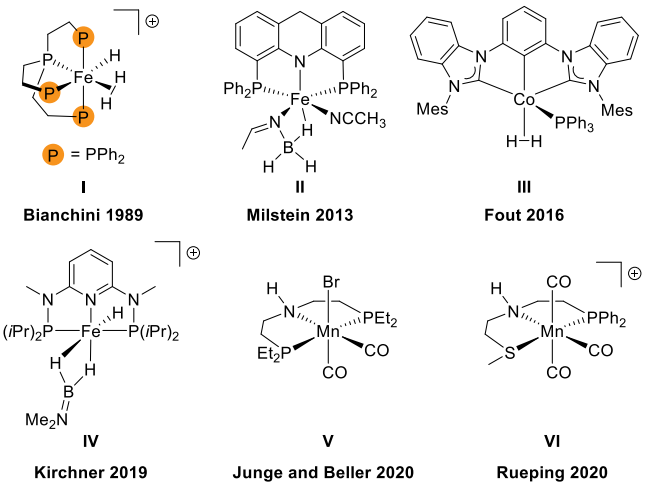

Figure 1. Selected examples of homogeneous, non-noble metal (pre)catalysts for the semihydrogenation of alkynes.

(*Z*)-alkene is formed first and then isomerized. Cationic PNP iron(II) complex **IV** published by the group of Kirchner efficiently hydrogenates internal alkynes to (*Z*)-alkenes under mild conditions.[11] Recently, our group published the first homogeneous manganese complex for the semihydrogenation

Special Issue: Sustainable Organometallic Chemistry

Received: December 21, 2021
Published: March 15, 2022

of alkynes.[12] Here, PNP manganese(I) complex **V** reduces diphenylacetylene derivates under mild conditions with excellent (*Z*)-selectivity. Mechanistic investigations revealed that hydrogenation proceeds via an outer-sphere mechanism utilizing the amino moiety in the ligand backbone for metal–ligand cooperativity[21] as it is often observed for these systems. No isomerization of the formed alkene takes place under the chosen conditions. Shortly after, Rueping and co-workers reported a similar cationic PNS manganese(I) complex **VI**.[13] This air-stable complex hydrogenates a variety of alkynes to the (*Z*)-alkenes under mild conditions.

Besides first-row transition metals, molybdenum also represents an attractive substitute for noble metals due to its low costs and toxicity.[22] Indeed, heterogeneous molybdenum catalysts are widely used for hydrogenation reactions[23] and homogeneous molybdenum complexes were studied for hydrogenations, particularly of N_2 and CO_2.[24−31] However, reports on catalytic hydrogenations with molybdenum complexes remain scarce in comparison to first-row transition metals.[32−38]

Our group has recently developed a series of structurally related low-valent molybdenum complexes as catalysts for the hydrogenation of ketones,[39] alkenes,[39] formamides,[40] and nitriles.[41] Based on this work, we became interested to explore their potential as catalysts for the semihydrogenation of alkynes.

RESULTS AND DISCUSSION

Synthesis and Characterization of Mo Complexes. Initially, a series of low-valent molybdenum complexes have been prepared starting from $Mo(CH_3CN)_2(CO)_2(PPh_3)_2$ (**1**) and the corresponding PNP ligands (Scheme 1, Figure 2)

Scheme 1. General Synthesis of Low-Valent PNP Molybdenum Complexes Used in This Work

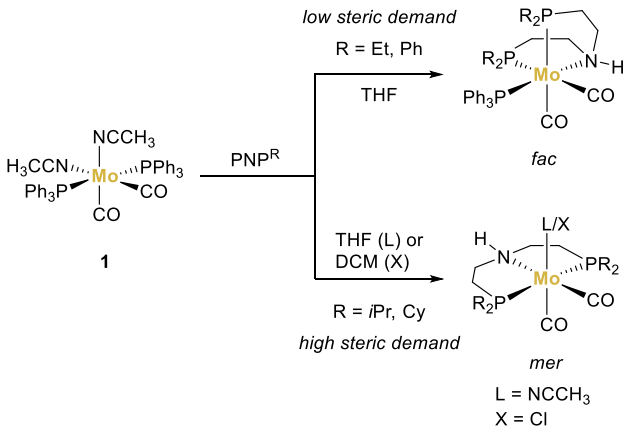

according to previous protocols.[39−41] Sterically low demanding substituents (Ph, Et) on the phosphines of the pincer ligand lead to complexes with a facial coordination mode of the PNP ligand. In these complexes a PPh_3 ligand remains besides the two strongly bound CO ligands on the Mo atom.

Increased steric demand on the phosphines (*i*Pr, Cy) causes a meridional arrangement of the PNP ligand, leading to the formation of more classical pincer complexes. Due to the structure of **1**, in which the weak-field CH_3CN ligands are located *trans* to the strong-field CO ligands, a meridional coordination of the PNP ligand inevitably results in the preservation of one CH_3CN ligand in the complex sphere. If

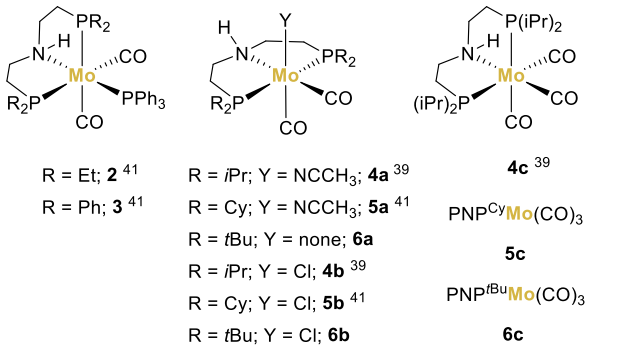

Figure 2. Series of molybdenum complexes tested in this work as catalysts for the semihydrogenation of alkynes.

the synthesis of these complexes is performed in DCM as a solvent, chlorinated molybdenum(I) complexes are obtained, in which the neutral CH_3CN ligand is replaced by a formally anionic Cl ligand.[39,41] The facially coordinated Ph-substituted complex **3** is more stable to chlorination and therefore can be prepared in DCM at room temperature. However, refluxing in DCM yields a heptacoordinated Mo(II) complex bearing two Cl ligands.[41] The reaction of the PNP^{Et} ligand and **1** in DCM leads to product mixtures even at −20 °C.[41]

The new complex **6a** was prepared according to Scheme 2. In contrast to the known *i*Pr- and Cy-substituted congeners,

Scheme 2. Synthesis of *t*Bu-Substituted PNP Molybdenum Complexes 6a, 6b, and 6c

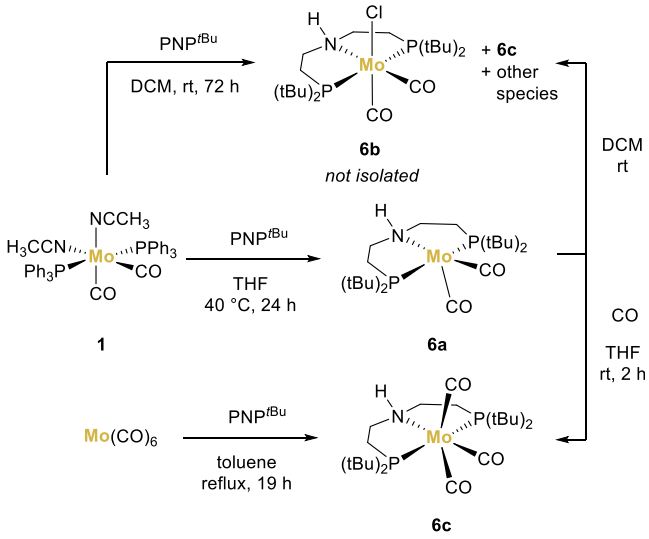

the conversion is not complete after stirring a solution of **1** and the PNP^{tBu} ligand at room temperature overnight, but increased temperature and/or longer reaction times were necessary (e.g., 40 °C for 24 h). Compound **6a** is sparingly soluble in common solvents (toluene, THF, acetonitrile, methanol, DMSO), and therefore, no crystals of the complex nor a meaningful NMR spectrum was obtained. Hence, **6a** could only be analyzed by IR spectroscopy and elemental analysis. The IR spectrum of **6a** features strong CO absorption bands at similar energies as observed for its *i*Pr- and Cy-substituted congeners **4a** and **5a**. However, no CN-stretch of a potential CH_3CN ligand was detected. Elemental analysis of the obtained material also pointed toward the absence of a CH_3CN ligand. This might be rationalized by the high steric

https://doi.org/10.1021/acs.organomet.1c00709
Organometallics 2022, 41, 1797−1805

demand of the *t*Bu-groups leaving little space in the coordination sphere.

If compound **1** is reacted with the PNP^{tBu} ligand in DCM or **6a** is dissolved in this solvent, formation of another complex was observed by IR spectroscopy, which proofed as a useful tool due to the strong CO absorption bands that all these complexes exhibit (see Supporting Information (SI) for details). However, attempts to isolate this compound in analytical purity remained unsuccessful. Most likely, molybdenum(I) complex **6b** is formed, as can be concluded from the observed reactivity of the analogous complexes **4a** and **5a** in DCM and the similarity of the IR spectrum of the formed complex with these of complexes **4b** and **5b**. In solution (THF, DCM, DMSO) **6a** and **6b** slowly form the tri(carbonyl)complex **6c** and other unidentified species.

Complex **6c** could be separately prepared by refluxing $Mo(CO)_6$ with a slight excess of PNP^{tBu} in toluene for 19 h. Furthermore, **6c** is obtained by the exposure of a suspension of complex **6a** in THF to CO gas, visible by a color change from brown red to yellow in a couple of minutes (see SI for images). The complex crystallizes as fine yellow needles from DCM/heptane, which were suitable for single crystal X-ray diffraction analysis. In the solid state of **6c** (Figure 3) the PNP ligand

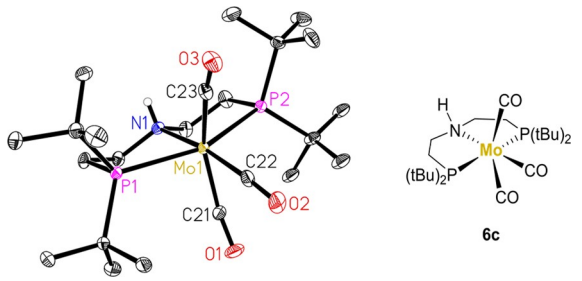

Figure 3. Molecular structure of **6c** in the solid-state. Displacement ellipsoids set at 30% probability level, carbon-bound hydrogen atoms and lower occupied atoms of the disordered *t*Bu-group are omitted for clarity. Selected bond lengths [Å] and angles [deg]: Mo1−N1 2.3582(14), Mo1−P1 2.5182(4), Mo1−C21 1.9963(19), Mo1−C22 1.9289(18), Mo1−C23 2.0042(19), C21−O1 1.166(2), C22−O2 1.179(2), C23−O3 1.161(2), N1−Mo1−C21 93.88(7), N1−Mo1−C22 168.91(7), N1−Mo1−C23 112.31(6), P1−Mo1−P2 154.23(2), C21−Mo1−C23 153.79(8).

coordinates meridionally to the molybdenum center, forcing two CO ligands in a *trans* position. This leaves the complex in a strongly distorted octahedral geometry with a C21−Mo1−C23 angle of 153.79(8)°, far from linearity.

The meridional structure of **6c** contrasts with the solid-state structure of the *i*Pr-substituted tri(carbonyl)molybdenum complex **4c**, which was found to have a facial ligand geometry.[39] The NMR spectra of complexes **4c**, **5c**, and **6c** show the presence of two different species whose ratio is solvent dependent.[42] Likely, in solution an equilibrium exists between the facial and the meridional complexes.

The resonance of the *t*Bu-groups of **6c** in the ^{1}H NMR spectrum shows a complex coupling pattern due to ^{1}H−^{31}P coupling. Decoupling of ^{31}P simplifies the resonances to two singlets in accordance with the C_S symmetry of the complex.

Next to Mo PNP pincer compounds, the coordination of NNP ligands to molybdenum was studied. Complex (*rac*)-**7** can easily be prepared by stirring **1** with a slight excess of the NNP ligand in THF at room temperature. In contrast to the symmetric PNP pincer complexes, which all feature a mirror plane, (*rac*)-**7** exhibits helical chirality due to the unsymmetric NNP ligand. In the solid state, the NNP ligand coordinates facially to the molybdenum center with the phosphine moiety being located *trans* to the one remaining PPh_3 ligand (Figure 4). The facial structure can be explained by the low steric

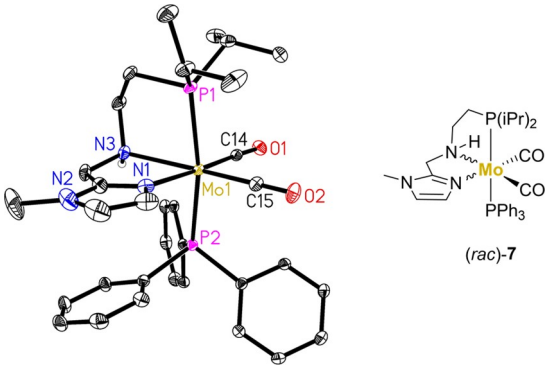

Figure 4. Molecular structure of (*rac*)-**7** in the solid-state. Displacement ellipsoids set at 30% probability level; carbon-bound hydrogen atoms omitted for clarity. Selected bond lengths [Å] and angles [deg]: Mo1−N1 2.2619(15) Mo1−N3 2.3839(14), Mo1−P1 2.4519(5), Mo1−P2 2.4347(5), Mo1−C14 1.9203(18), Mo1−C15 1.9202(17), C14−O1 1.190(2), C15−O2 1.185(2), N1−Mo1−N3 72.92(5), P1−Mo1−P2 168.83(2), N1−Mo1−C14 176.41(6), N3−Mo1−C15 169.17(6).

demand of the *N*-methylimidazolyl group (compare Scheme 1). Interestingly, in (*rac*)-**7** the PPh_3 ligand is located *trans* to the phosphine of the NNP ligand, whereas in **2** and **3** it opposes the amino functionality of the PNP ligand. However, heating a solution of **3** in toluene-d_8 to 80 °C leads to a mixture of complexes as indicated by NMR experiments. One of the formed complexes likely is a complex (*iso*)-**3** in which the PPh_3 ligand is opposing a phosphine of the PNP ligand in analogy to the solid-state structure of (*rac*)-**7** (see SI for details). Also, resonances that can be assigned to meridional complexes were observed, indicating that *fac-mer* isomerization takes places at elevated temperatures. Due to the helical chirality of (*rac*)-**7**, protons bound to the same carbon atom in the methylene and ethylene linker in the ligand backbone as well as the two *i*Pr-groups are diastereotopic to each other. Together with the limited solubility of (*rac*)-**7**, this leads to a low intensity of the resonances of these protons in the ^{1}H NMR spectrum. As expected, the ^{31}P NMR spectrum of (*rac*)-**7** in CD_3CN exhibits two doublets at 67.24 and 55.54 ppm, respectively. Furthermore, some free PPh_3 is observed which originates from the complex, since no resonance for free PPh_3 is found for a suspension of (*rac*)-**7** in toluene-d_8, in which (*rac*)-**7** itself is insoluble. This implies that PPh_3 is not strongly bound in (*rac*)-**7**.

The IR spectrum of (*rac*)-**7** exhibits two strong CO absorption bands at 1778 and 1697 cm^{-1}. The very low energy of the absorptions—being in the area typically observed for C═O double bonds—displays the strong π-backbonding to the CO ligands and the electron richness of the complex. For comparison, complexes **2** and **3** show CO absorptions at higher energies (1812, 1730 cm^{-1} and 1827, 1743 cm^{-1}, respectively)[41] which illustrates the weaker electron-donating ability of the phosphines compared with the *N*-methylimida-

https://doi.org/10.1021/acs.organomet.1c00709
Organometallics 2022, 41, 1797−1805

zolyl group. Liu and co-workers observed similar ligand properties with analogous manganese complexes.[43]

Catalytic Hydrogenation of Diphenylacetylene with Low-Valent Molybdenum Complexes. We started our catalytic experiments by investigating the different molybdenum(0) and molybdenum(I) complexes as catalysts for the hydrogenation of alkynes (Table 1). Diphenylacetylene was reacted as a model substrate under 30 bar of H_2 pressure at 80 °C using 5 mol % catalyst and 5 mol % $NaHBEt_3$ as base, since $NaHBEt_3$ has significantly affected catalyst activity in previous works.[39−41]

Table 1. Molybdenum-Catalyzed Hydrogenation of Diphenylacetylene[a]

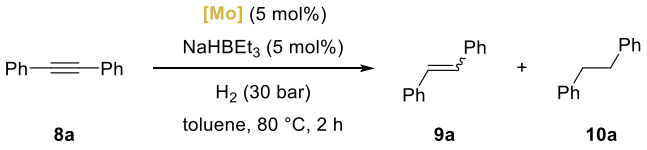

Entry	[Mo]	Conv[b]	Yield **9a** (%)	(*Z*)/(*E*)	Yield **10a** (%)
1	**2**	17	15	36:64	2
2	**3**	54	51	57:43	3
3	**4a**	68	65	75:25	3
4	**4b**	14	7	76:24	7
5	**5a**	93	89	85:15	4
6	**5b**	7	2	n.d.	5
7	**6a**	1	1	n.d.	0
8	**6c**	3	2	n.d.	1
9	(*rac*)-**7**	19	15	77:23	4
10	**1**	21	13	33:67	8
11	none	1	1	n.d.	0

[a]Reaction conditions: 0.5 mmol of **8a**, a 0.5 M solution of $NaHBEt_3$ in toluene and 2 mL of toluene were used. [b]Conversion, yield, and (*Z*)/(*E*) ratio were determined by GC analysis using hexadecane as internal standard.

The facial complexes **2** and **3** showed mediocre conversions and diastereoselectivities (Table 1, entries 1−2), whereas the meridional complexes **4a** and **5a** performed better especially regarding the diastereoselectivity (Table 1, entries 3 and 5). Complex **5a** gave the best results with nearly full conversion (93%) and a good diastereoselectivity of 85:15 in favor of the (*Z*)-diastereomer. In contrast, the chlorinated molybdenum(I) complexes **4b** and **5b** only showed low conversions.

Interestingly, the observed difference in catalytic activity between **4a** and **5a** was surprisingly large (93% to 68% conversion). Since the electronic properties of the *i*Pr- and the Cy-substituents are quite similar, we suggest that the improved catalytic activity might be caused by the increased steric demand.

To prove this assumption the *t*Bu-substituted PNP complexes **6a** and **6c** were tested in the semihydrogenation of diphenylacetylene. Unfortunately, both complexes, **6a** and **6c**, showed nearly no catalytic activity (Table 1, entries 7−8).

For related Mn-complexes, NNP-type ligands showed an improved catalytic activity in hydrogenation reactions in comparison to the PNP complexes.[43,44] Therefore, the respective Mo NNP pincer complex (*rac*)-**7** (*vide supra*) was tested under our standard conditions. However, complex (*rac*)-**7** showed moderate conversion and good diastereoselectivity (Table 1, entry 9). By applying complex **1**, moderate conversion and diastereoselectivity were obtained (Table 1, entry 10), and by just using $NaHBEt_3$ without a molybdenum complex, no conversion of diphenylacetylene was observed (Table 1, entry 11).

Variation of the Reaction Conditions and Substrate Scope of the Semihydrogenation. After identifying complex **5a** as the most promising precatalyst, we investigated the influence of different reaction parameters such as solvents and bases on the outcome of the reaction (Table 2). Polar solvents like THF, acetonitrile, or DCM led to poor conversions (<10%), whereas nonpolar, aprotic solvents like toluene, cyclohexane, and heptane are suitable for the reaction. Both toluene and cyclohexane provided high conversions and yields around 90% (Table 2, entries 1 and 3). In the base screening, $NaHBEt_3$ presented the best results under the tested conditions (Table 2, entry 1). For NaHMDS a slightly lower conversion and yield were observed (Table 2, entry 7). The weaker bases $NaHBH_3$, NaOH, and NaO*t*Bu gave only low conversions (≤10%) (Table 2, entries 8−10), which are comparable with the results obtained without addition of base (Table 2, entry 11).

Table 2. Influence of Solvent and Base on the Molybdenum-Catalyzed Hydrogenation of Diphenylacetylene[a]

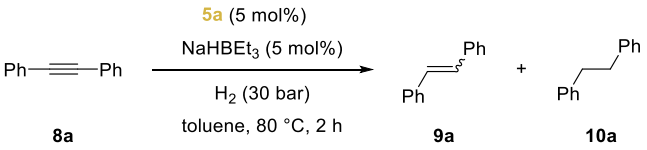

Entry	Deviation	Conv[b]	Yield **9a** (%)[b]	(*Z*)/(*E*)	Yield **10a** (%)[b]
1	–	93	89	85:15	4
2	THF	9	4	68:32	5
3	heptane	46	44	73:27	2
4	acetonitrile	1	1	n.d.	0
5	DCM	3	1	n.d.	2
6	cyclohexane	92	87	86:14	5
7	NaHMDS	79	75	87:13	4
8	$NaHBH_3$	9	5	58:42	4
9	NaOH	9	5	52:48	4
10	NaO*t*Bu	10	4	45:55	6
11	no base	9	4	43:57	5

[a]Reaction conditions: 0.5 mmol of **8a**, a 0.5 M solution of $NaHBEt_3$ in toluene and 2 mL of toluene were used. [b]Conversion, yield, and (*Z*)/(*E*) ratio were determined by GC analysis using hexadecane as internal standard.

Thus, a strong base seems to be needed to form the active catalyst species, likely an anionic amido complex which is generated by the deprotonation of the amine in the ligand backbone.[40] Interestingly, variation of the cation of the additive has a significant influence on the catalytic performance. While $LiHBEt_3$ showed lower activity (32% conv, 23% yield, 84:16 (*Z*)/(*E*)) in comparison to $NaHBEt_3$, $KHBEt_3$ produced comparable conversion and yield but lower diastereoselectivity (84% conv, 79% yield, 73:27 (*Z*)/(*E*)). The influence of the cation is further supported by experiments in the presence of 15-crown-5, which is known to selectively bind potassium ions (see SI for details). A similar effect was found for the addition of THF.

Furthermore, catalyst loading, reaction temperature, and the dihydrogen pressure were investigated (Table 3). Even a slight decrease of the catalyst loading resulted in a major loss in conversion and yield (Table 3, entries 2−3). At 60 °C the

https://doi.org/10.1021/acs.organomet.1c00709
Organometallics 2022, 41, 1797−1805

Table 3. Influence of Catalyst Loading, Temperature and Dihydrogen Pressure on the Molybdenum-Catalyzed Hydrogenation of Diphenylacetylene[a]

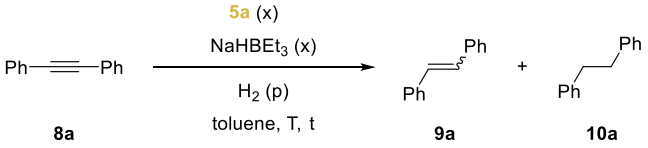

8a 9a 10a

Entry	x [mol %]	T [°C]	p [bar]	t [h]	Conv[b]	Yield **9a**[b] (%)	$(Z)/(E)$	Yield **10a**[b] (%)
1	5.0	80	30	2	93	89	85:15	4
2	4.0	80	30	2	64	61	86:14	3
3	2.5	80	30	2	11	7	51:49	4
4	5.0	60	30	2	71	68	85:15	3
5	5.0	60	30	6	98	96	86:14	3
6	5.0	80	20	2	81	79	86:14	2
7	5.0	80	10	2	39	32	84:16	7
8[c]	5.0	80	30	2	98	96	86:14	4

[a]Reaction conditions: 0.5 mmol of **8a**, a 0.5 M solution of $NaHBEt_3$ in toluene and 2 mL of toluene were used. [b]Conversion, yield, and $(Z)/(E)$ ratio were determined by GC analysis using hexadecane as internal standard. [c]1 mL instead of 2 mL of toluene as solvent.

reaction proceeded slower, but by applying longer reaction times, full conversion could be reached (Table 3, entries 4−5). Under 20 bar of dihydrogen pressure, a slight decrease in conversion and yield is obtained, and lowering the pressure to 10 bar results in much lower conversion and yield (Table 3, entries 6−7). Conversion and yield could be enhanced by running the reaction at higher concentrations (Table 3, entry 8). During all these variations of parameters, the diastereoselectivity was not influenced.

Next, various substituted diphenylacetylenes were reacted under the optimized reaction conditions (Scheme 3). While a methyl substitution in the para- (**8b**) or meta-position (**8c**) on one of the phenyl rings was well tolerated and showed no significant difference compared to diphenylacetylene **8a**, methylation in the ortho-position (**8d**) resulted in drastically lowered conversion but similar diastereoselectivity. Fluorine-containing substrate **8e** was smoothly converted to the corresponding alkene **9e** with good diastereoselectivity, whereas for the more reactive chloride **8f** and bromide **8g**, small amounts of hydrodehalogenation products were observed. Likely, the catalyst is deactivated by halogenation in these cases, resulting in lower conversions and yields.

Electron-rich substituted diphenylacetylenes (**8h−k**) including ethers, thioethers, and silanes were readily converted to the corresponding alkenes (**9h−k**). Under standard reaction conditions (80 °C, 2 h) in all cases small amounts (>10%) of alkane were observed. By applying lower temperatures at an increased reaction time (60 °C, 16 h), reduction to the alkane could mostly be suppressed and high yields (91−86%) as well as good diastereoselectivities (91:9−79:21) were obtained.

For diphenylacetylenes featuring electron-withdrawing substituents like nitriles and ketones as well as nitro, ester, or trifluoromethyl groups, only low conversions (≥10%) were observed (see SI for detailed results). Even when a strongly electron-donating methoxy group is present, a trifluoromethyl group on the other phenyl ring, like in substrate **8m**, resulted in a low conversion. A possible explanation might be that the catalyst is inhibited by the substrates through the formation of stable alkyne complexes. A similar effect was observed for the pyridine derivative **8q** (see SI). Diyne **8p** featuring two directly connected alkyne functionalities resulted in poor conversion and yield (see SI), whereas substrate **8n** could be easily converted to the corresponding diene with a selectivity of the (Z, Z)-diastereomer **9n** to the other diastereomers of 86:14. Although sulfur-containing compounds often completely block hydrogenation catalysts, the thiophene-containing substrate **8o** showed moderate conversion.

Besides aryl−aryl alkynes also terminal alkynes, as well as aryl-alkyl or alkyl−alkyl alkynes, were tested. Unfortunately, all these substrate classes showed only low conversions under the applied conditions in the presence of either **4a** or **5a** as catalyst (see SI).

Finally, a series of mechanistic control experiments were performed. To investigate if isomerization of the formed alkenes takes place during the reaction, (Z)- and (E)-stilbene were used as starting material, respectively (Scheme 4). When (E)-stilbene was used, no significant isomerization and only traces of alkane were observed. In the case of (Z)-stilbene, formation of 2% of the more stable (E)-isomer and of the alkane were detected, respectively. This clearly shows that isomerization reactions are no major pathway under these conditions. Next, to examine whether metal−ligand cooperativity (MLC) is involved, the free NH-moiety in the ligand backbone of **4a** was blocked by substitution. When the *N*-methylated derivative **4a-Me** was applied under standard conditions, no significant hydrogenation occurred indicating an outer-sphere mechanism including MLC. Also, when **5a** was used with 5 mol % of PPh_3 as an additive under standard conditions (see SI for details), no decrease in catalytic activity was found, as would be expected for an inner-sphere mechanism due to the blocking of a vacant coordination site. This further supports an outer-sphere mechanism for the described hydrogenation reactions.

SUMMARY AND CONCLUSIONS

Here, we describe novel homogeneous catalytic hydrogenation of alkynes using molybdenum complexes. The new *t*Bu substituted Mo PNP pincer complexes **6a** and **6c** as well as the NNP pincer complex (*rac*)-**7** have been prepared and characterized. These complexes as well as related complexes were tested as catalysts in the semihydrogenation of diphenylacetylene. The best performance was obtained in the presence of the cyclohexyl-substituted complex **5a** $PNP^{Cy}Mo(CO)_2(CH_3CN)$. Utilizing this catalyst, various internal diaryl alkynes are hydrogenated to the corresponding alkenes with good to very good chemo- and diastereoselectivity for the (Z)-

https://doi.org/10.1021/acs.organomet.1c00709
Organometallics 2022, 41, 1797−1805

Scheme 3. Molybdenum Catalyzed Semihydrogenation of Selected Alkyne Substrates[a]

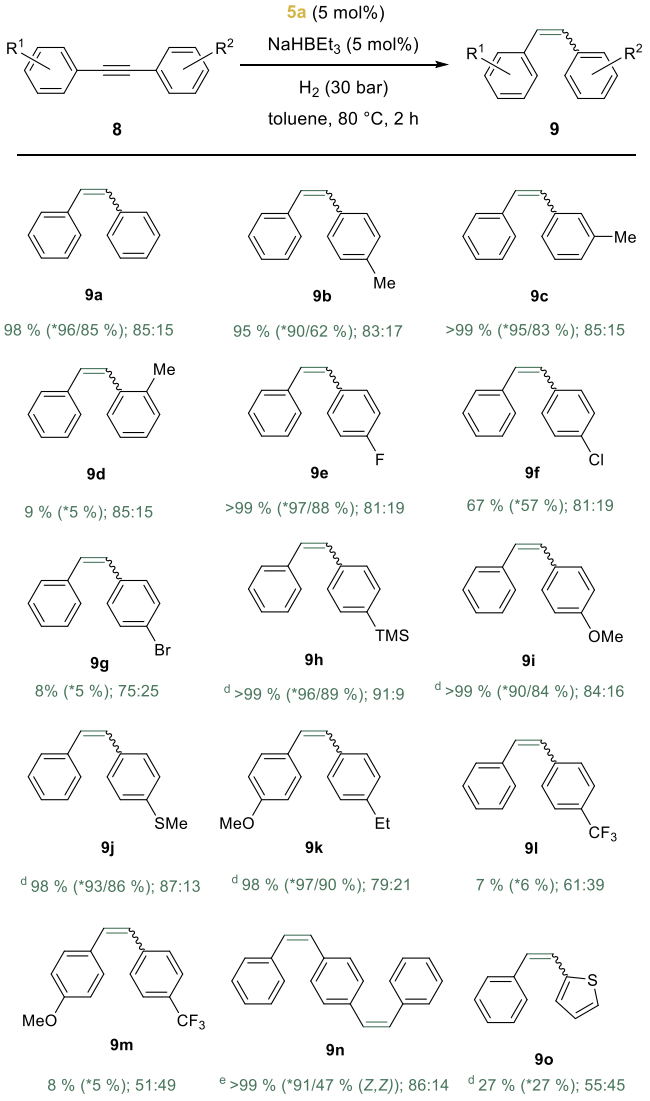

[a]Reaction conditions: 0.5 mmol of **8**, a 0.5 M solution of $NaHBEt_3$ in toluene and 1 mL of toluene were used. [b]Conversion and (*Z*)/(*E*) ratio were determined by GC analysis. [c]Yield determined by GC analysis; isolated yield given in brackets. [d]60 °C, 16 h. [e]GC yield for all diastereomers, isolated yield for (*Z*, *Z*) diastereomer, diastereomeric ratio of (*Z*, *Z*) to other diastereomers.

alkene and no significant isomerization taking place. However, the tolerance of this catalytic system toward substrates with electron-withdrawing substituents is limited, allowing for further improvement. Mechanistic experiments pointed toward an outer-sphere mechanism including MLC.

EXPERIMENTAL SECTION

General Information. All manipulations, except when indicated otherwise, were carried out under an argon atmosphere with exclusion of air and moisture using standard Schlenk and glovebox techniques. Solvents were dried over activated alumina columns using a solvent purification system (Innovative Technology PS-MD-6) and stored over molecular sieves (4 Å) under an argon atmosphere. Deuterated solvents were purchased from eurisotop, degassed by three successive freeze−pump−thaw cycles, and stored over molecular sieves (4 Å) under an argon atmosphere. NMR spectra were recorded on a Bruker Avance (300 MHz, 400 MHz) or Bruker Fourier (300 MHz)

Scheme 4. Mechanistic Experiments Performed for the Molybdenum Catalyzed Semihydrogenation of Alkynes[a]

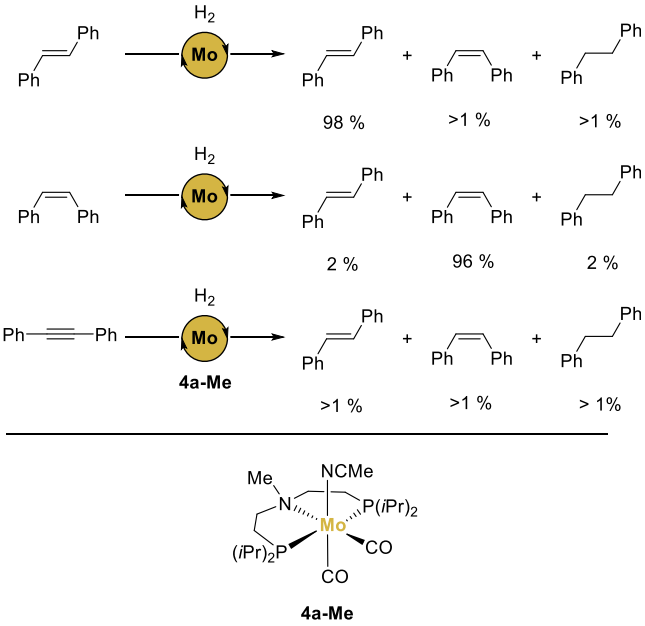

[a]Reaction conditions: 0.5 mmol of diphenylacetylene, (*Z*)-stilbene or (*E*)-stilbene as starting material, 5 mol % of molybdenum catalyst, a 0.5 M solution of $NaHBEt_3$ in toluene, 30 bar of dihydrogen pressure and 1 mL of toluene as a solvent were used at 80 °C for 2 h. [b]Yields were determined by GC analysis using hexadecane as an internal standard.

instrument. Chemical shifts (δ) are reported in parts per million (ppm) and are referenced to residual proton solvent signals or carbon resonances.[45,46] Infrared spectra were recorded in the solid state on a Nicolet iS 5 FT-IR spectrometer equipped with a PIKE Technologies GladiATR ATR. Elemental analyses were carried out in the Microanalysis Laboratory of the institute on a Leco TruSpec Micro CHNS device. GC analyses were carried out on an Agilent 7890A chromatograph using an HP-5 column (30 m × 0.25 m × 0.25 m). Bis[2-(diphenylphosphino)ethyl]ammonium chloride (15-7306), bis-[2-(di-isopropylphosphino)ethyl]amine (15-7304), and bis[2-(dicyclohexylphosphino)ethyl]amine (15-7310) were purchased from Strem Chemicals and used without further purification. Bis[2-(di-*tert*-butylphosphino)ethyl]amine (AB393139) was purchased from abcr and used without further purification. Bis[2-(diethylphosphino)ethyl]amine[47] and 2-(di-isopropylphosphino)-*N*-((1-methyl-1*H*-imidazol-2-yl)methyl)ethylamine[48] were synthesized according to literature. $NaHBEt_3$ was purchased from Sigma-Aldrich (227307). $Mo(CO)_6$ was purchased from Sigma-Aldrich (577766) with a metal purity of ≥99.9%. The complexes **1**,[49−51] **2**,[41] **3**,[41] **4a**,[39] **4a-Me**,[42] **4b**,[39] **5a**,[41] and **5b**[41] were synthesized according to literature procedures.

*Synthesis of $Mo(CH_3CN)_2(CO)_2(PPh_3)_2$ (**1**).* The procedure was adapted from literature.[49−51] In a 500 mL three-necked round-bottom equipped with a large stirring bar and a reflux condenser, $Mo(CO)_6$ (5.07 g, 19.2 mmol, 1.0 equiv) was suspended in 40 mL of acetonitrile and 40 mL of benzene and heated to reflux (95 °C oil bath temperature) for 4 h. The reaction mixture was allowed to cool to room temperature, and allylbromide (2.32 g, 19.2 mmol, 1.0 equiv) was added dropwise resulting in a color change from yellow to red. The mixture was heated to reflux for another 19 h, and an orange solid precipitated upon cooling to room temperature. The solution was filtered off at 0 °C, and the residue was suspended in 60 mL of acetonitrile. Triphenylphosphine (15.11 g, 57.61 mmol, 3.0 equiv) was added in one portion resulting in a color change to red. Upon heating to reflux for 2 h, a yellow solid precipitated. After cooling to room temperature, the solution was filtered off and the residue was

https://doi.org/10.1021/acs.organomet.1c00709
Organometallics 2022, 41, 1797−1805

thoroughly washed with acetonitrile (3 × 20 mL) and dried *in vacuo*, yielding **1** as a light-yellow solid (9.95 g, 68%). $^{31}P\{^{1}H\}$ NMR (161.99 MHz, DMSO-d_6, 295 K): δ [ppm] = 54.75 (s), 52.04 (s), 50.29 (s), 36.77 (s) 25.46 (s). Multiple resonances are observed because of ligand exchange with DMSO. Therefore, a resonance at −6.9 ppm is observed which is assigned to free PPh_3. A clear assignment of the resonances to the different formed complexes was not performed. Data are still provided for comparison. IR (ATR): ν [cm^{-1}] = 1806 (CO), 1734 (CO).

*Synthesis of $PNP^{Cy}Mo(CO)_3$ (**5c**).* In a 25 mL Schlenk tube $Mo(CO)_6$ (150.0 mg, 568 μmol, 1.0 equiv) and bis[2-(dicyclohexylphosphino)ethyl]amine (277.8 mg, 596.6 μmol, 1.05 equiv) were dissolved in 10 mL of toluene. The reaction mixture was heated to reflux for 19 h. The orange suspension was allowed to cool to room temperature. The solvent was filtered off, and the residue was washed with toluene (2 × 2 mL) and heptane (2 × 2 mL). The light-yellow solid was dried *in vacuo* (311.0 mg, 89%). ^{1}H NMR (400.13 MHz, CD_2Cl_2, 295 K): δ [ppm] = 3.22−3.05 (m, 2H), 2.77−1.10 (m, 49H), 0.84−0.68 (m, 2H). $^{31}P\{^{1}H\}$ NMR (161.99 MHz, CD_2Cl_2, 295 K): δ [ppm] = 65.67 (s), 41.43 (s). Elemental Analysis Calcd for $C_{31}H_{53}MoNO_3P_2$: C, 57.67; H, 8.27; N, 2.17. Found: C, 57.57; H, 8.64; N, 1.99. IR (ATR): ν [cm^{-1}] = 1897 (CO), 1795 (CO), 1761 (CO).

*Synthesis of $PNP^{tBu}Mo(CO)_2$ (**6a**).* In a 25 mL Schlenk tube $Mo(CH_3CN)_2(CO)_2(PPh_3)_2$ (199.9 mg, 263 μmol, 1.0 equiv) was suspended in 5 mL of THF, bis[2-(di-*tert*-butylphosphino)ethyl]-amine (10 wt % in toluene, 100.0 mg, 277 μmol, 1.05 equiv) was added, and the reaction mixture was heated at 40 °C for 20 h. The reaction mixture was allowed to cool to room temperature, the solvent was filtered off, and the red-brown residue was washed with THF (4 × 2 mL). Drying in vacuo yielded **6a** as a red solid (145.1 mg, quant.). Elemental Analysis Calcd for $C_{22}H_{45}MoNO_2P_2$: C, 51.46; H, 8.83; N, 2.73. Found: C, 52.48; H, 8.59; N, 1.78. Although these results are outside the range viewed as establishing analytical purity, they are provided to illustrate the best values obtained to date. IR (ATR): ν [cm^{-1}] = 1769 (CO), 1677 (CO).

*Synthesis of $PNP^{tBu}Mo(CO)_3$ (**6c**).* **From 6a:** In a 25 mL Schlenk tube **6a** (110 mg, 214 μmol, 1.0 equiv) was suspended in 5 mL of THF. CO gas was introduced into the suspension, and a color change from brown red to yellow was observed within minutes. After 2 h, all volatiles were removed in vacuo yielding **6c** as a yellow solid (116 mg, quant.). **From $Mo(CO)_6$:** In a 25 mL Schlenk tube $Mo(CO)_6$ (148.3 mg, 562 μmol, 1.0 equiv) was dissolved in 10 mL of toluene and bis[2-(di-*tert*-butylphosphino)ethyl]amine (10 wt % in THF, 213.0 mg, 590 μmol, 1.05 equiv) was added. The reaction mixture was heated to reflux for 19 h. The red-brown suspension was allowed to cool to room temperature. The solvent was filtered off, and the residue was washed with toluene (2 × 1 mL). The residue was dissolved in DCM, and a yellow solid precipitated by adding heptane. The solvent was filtered off, and the residue was washed with heptane (2 × 2 mL). Drying *in vacuo* yielded **6c** as a yellow solid (190 mg, 63%). Yellow needles suitable for single-crystal X-ray diffraction were obtained by slow diffusion of heptane into a solution of **6c** in DCM at 0 °C. ^{1}H NMR (300.20 MHz, CD_2Cl_2, 295 K): δ [ppm] = 3.40−3.20 (m, 2H), 2.46−2.19 (m, 3H), 2.18−2.05 (m, 2H), 1.60−1.41 (m, 2H), 1.39−1.30 (m, 36H). $^{1}H\{^{31}P\}$ NMR (400.13 MHz, CD_2Cl_2, 295 K): δ [ppm] = 3.34−3.27 (m, 2H), 2.43−2.21 (m, 3H), 2.15−2.07 (m, 2H), 1.55−1.44 (m, 2H), 1.35 (s, 18H), 1.34 (s, 18H). $^{31}P\{^{1}H\}$ NMR (121.52 MHz, CD_2Cl_2, 295 K): δ [ppm] = 101.96 (s). Elemental Analysis Calcd for $C_{23}H_{45}MoNO_3P_2$: C, 51.01; H, 8.38; N, 2.59. Found: C, 51.08; H, 8.45; N, 2.41. IR (ATR): ν [cm^{-1}] = 1904 (CO), 1782 (CO), 1761 (CO).

*Synthesis of $NNP^{iPr}Mo(CO)_2(PPh_3)$ ((rac)-**7**).* In a 25 mL Schlenk tube $Mo(CH_3CN)_2(CO)_2(PPh_3)_2$ (569.3 mg, 750 μmol, 1.0 equiv) was suspended in 15 mL of THF, 2-(di-isopropylphosphino)-*N*-((1-methyl-1*H*-imidazol-2-yl)methyl)ethylamine (10 wt % in toluene, 210.8 mg, 826 μmol, 1.1 equiv) was added, and the reaction mixture was stirred at room temperature for 22 h. The solvent was filtered off, and the yellow residue was washed with hexane (5 × 5 mL). Drying *in vacuo* yielded (*rac*)-**7** as a yellow solid (403 mg, 80%). Red crystals suitable for single-crystal X-ray diffraction were obtained by slow diffusion of Et_2O into a solution of (*rac*)-**7** in acetonitrile at 0 °C. ^{1}H NMR (300.20 MHz, CD_3CN, 295 K): δ [ppm] = 7.61−7.52 (m, 6H), 7.33−7.21 (m, 9H), 6.62−6.58 (m, 2H), 3.32 (bs, 1H), 3.23 (s, 3H), 3.17−3.09 (m 1H), 2.86−2.61 (m, 3H), 2.40−2.56 (m, 1H), 1.82−1.68 (m, 1H), 1.39−1.17 (m, 10H), 1.09−0.99 (m, 4H). ^{31}P NMR (121.52 MHz, CD_3CN, 295 K): δ [ppm] = 67.24 (d, J = 141 Hz), 55.54 (d, J = 141 Hz). IR (ATR): ν [cm^{-1}] = 1778 (CO), 1697 (CO).

General Procedure for Hydrogenation Experiments. All hydrogenation reactions were carried out in a 300 mL autoclave (Parr Instrument Company). In a glovebox a 4 mL glass vial was charged with the corresponding molybdenum catalyst and a stirring bar. Solvent and $NaHBEt_3$ (0.5 M in toluene) were subsequently added, and the reaction mixture was stirred for approximately 10 min. The corresponding alkyne was added, and the vial was closed with a screw cap containing a septum. The septum of the vial was punctured with a needle to allow for the exchange of atmosphere, and the vial was transferred into an autoclave. The sealed autoclave was purged ten times with 10 bar of pressure of dihydrogen gas before the desired pressure was set. The autoclave was heated in a preheated aluminum block for the desired reaction time. Afterward, the autoclave was cooled in an ice bath and carefully depressurized. The reaction mixture was diluted with ethyl acetate, a known amount of hexadecane was added as an internal standard, and the mixture was filtered through a pad of Celite.

■ ASSOCIATED CONTENT

Supporting Information

The Supporting Information is available free of charge at https://pubs.acs.org/doi/10.1021/acs.organomet.1c00709.

Screening of reaction conditions. Results of hydrogenation experiments for alkynes **8p**−**8aa**. Analytical data and NMR spectra of isolated alkenes. Photographs of the reaction of **6a** with CO to **6c**. NMR and IR spectra of the material obtained by the reaction of **1** with ^{tBu}PNP in DCM. NMR and IR spectra of **1**, **5c**, **6a**, **6c**, and (*rac*)-**7**. Crystallographic details for molecular structures of **6c** and (*rac*)-**7**. (PDF)

Accession Codes

CCDC 2129493−2129494 contain the supplementary crystallographic data for this paper. These data can be obtained free of charge via www.ccdc.cam.ac.uk/data_request/cif, or by emailing data_request@ccdc.cam.ac.uk, or by contacting The Cambridge Crystallographic Data Centre, 12 Union Road, Cambridge CB2 1EZ, UK; fax: +44 1223 336033.

■ AUTHOR INFORMATION

Corresponding Authors

Matthias Beller − *Leibniz-Institut für Katalyse e.V., 18059 Rostock, Germany;* orcid.org/0000-0001-5709-0965; Email: matthias.beller@catalysis.de

Kathrin Junge − *Leibniz-Institut für Katalyse e.V., 18059 Rostock, Germany;* orcid.org/0000-0001-7044-8888; Email: kathrin.junge@catalysis.de

Authors

Niklas F. Both − *Leibniz-Institut für Katalyse e.V., 18059 Rostock, Germany*

Anke Spannenberg − *Leibniz-Institut für Katalyse e.V., 18059 Rostock, Germany*

Complete contact information is available at: https://pubs.acs.org/10.1021/acs.organomet.1c00709

Notes

The authors declare no competing financial interest.

■ ACKNOWLEDGMENTS

We gratefully acknowledge the support from the Federal Ministry of Education and Research of Germany, the state of Mecklenburg Western Pomerania, and the European Research Council (EU project 670986-NoNaCat). We thank Helen Hornke for experimental support and PD Dr. Wolfgang Baumann, Dr. Thomas Leischner, Johannes Fessler, and Florian Bourriquen for helpful discussions. Furthermore, we thank the analytical department of the Leibniz-Institute for Catalysis for analytical measurements.

■ REFERENCES

(1) Crespo-Quesada, M.; Cárdenas-Lizana, F.; Dessimoz, A.-L.; Kiwi-Minsker, L. Modern Trends in Catalyst and Process Design for Alkyne Hydrogenations. *ACS Catal.* **2012**, *2*, 1773−1786.

(2) Chen, B.; Dingerdissen, U.; Krauter, J.; Rotgerink, H. L.; Möbus, K.; Ostgard, D.; Panster, P.; Riermeier, T.; Seebald, S.; Tacke, T. New Developments in Hydrogenation Catalysis Particularly in Synthesis of Fine and Intermediate Chemicals. *Appl. Catal. A: Gen.* **2005**, *280*, 17−46.

(3) Negishi, E.-i.; De Meijere, A. *Handbook of Organopalladium Chemistry for Organic Synthesis*; John Wiley & Sons: 2003.

(4) Vilé, G.; Albani, D.; Almora-Barrios, N.; López, N.; Perez-Ramirez, J. Advances in the Design of Nanostructured Catalysts for Selective Hydrogenation. *ChemCatChem.* **2016**, *8*, 21−33.

(5) Lindlar, H. Palladium Catalyst for Partial Reduction of Acetylenes. *Org. Synth.* **1966**, *46*, 89−92.

(6) Ludwig, J. R.; Schindler, C. S. Catalyst: Sustainable Catalysis. *Chem.* **2017**, *2*, 313−316.

(7) Gregori, B. J.; Nowakowski, M.; Schoch, A.; Pöllath, S.; Zweck, J.; Bauer, M.; von Wangelin, A. J. Stereoselective Chromium-Catalyzed Semi-Hydrogenation of Alkynes. *ChemCatChem.* **2020**, *12*, 5359−5363.

(8) Bianchini, C.; Meli, A.; Peruzzini, M.; Vizza, F.; Zanobini, F.; Frediani, P. A Homogeneous Iron(II) System Capable of Selectively Catalyzing the Reduction of Terminal Alkynes to Alkenes and Buta-1,3-dienes. *Organometallics* **1989**, *8*, 2080−2082.

(9) Bianchini, C.; Meli, A.; Peruzzini, M.; Frediani, P.; Bohanna, C.; Esteruelas, M. A.; Oro, L. A. Selective Hydrogenation of 1-Alkynes to Alkenes Catalyzed by an Iron(II) cis-Hydride η^2-Dihydrogen Complex. A Case of Intramolecular Reaction between η^2-H_2 and σ-Vinyl Ligands. *Organometallics* **1992**, *11*, 138−145.

(10) Srimani, D.; Diskin-Posner, Y.; Ben-David, Y.; Milstein, D. Iron Pincer Complex Catalyzed, Environmentally Benign, *E*-Selective Semi-hydrogenation of Alkynes. *Angew. Chem., Int. Ed.* **2013**, *52*, 14131−14134.

(11) Gorgas, N.; Brünig, J.; Stöger, B.; Vanicek, S.; Tilset, M.; Veiros, L. F.; Kirchner, K. Efficient *Z*-Selective Semihydrogenation of Internal Alkynes Catalyzed by Cationic Iron(II) Hydride Complexes. *J. Am. Chem. Soc.* **2019**, *141*, 17452−17458.

(12) Garbe, M.; Budweg, S.; Papa, V.; Wei, Z.; Hornke, H.; Bachmann, S.; Scalone, M.; Spannenberg, A.; Jiao, H.; Junge, K. Chemoselective Semihydrogenation of Alkynes Catalyzed by Manganese(I)-PNP Pincer Complexes. *Catal. Sci. Technol.* **2020**, *10*, 3994−4001.

(13) Zubar, V.; Sklyaruk, J.; Brzozowska, A.; Rueping, M. Chemoselective Hydrogenation of Alkynes to (*Z*)-Alkenes Using an Air-Stable Base Metal Catalyst. *Org. Lett.* **2020**, *22*, 5423−5428.

(14) Tokmic, K.; Fout, A. R. Alkyne Semihydrogenation with a Well-Defined Nonclassical Co−H_2 Catalyst: A H_2 Spin on Isomerization and *E*-selectivity. *J. Am. Chem. Soc.* **2016**, *138*, 13700−13705.

(15) Chen, F.; Kreyenschulte, C.; Radnik, J. r.; Lund, H.; Surkus, A.-E.; Junge, K.; Beller, M. Selective Semihydrogenation of Alkynes with N-Graphitic-Modified Cobalt Nanoparticles Supported on Silica. *ACS Catal.* **2017**, *7*, 1526−1532.

(16) Lapointe, S.; Pandey, D. K.; Gallagher, J. M.; Osborne, J.; Fayzullin, R. R.; Khaskin, E.; Khusnutdinova, J. R. Cobalt Complexes of Bulky PNP Ligand: H_2 Activation and Catalytic Two-Electron Reactivity in Hydrogenation of Alkenes and Alkynes. *Organometallics* **2021**, *40*, 3617−3626.

(17) Thiel, N. O.; Kaewmee, B.; Ngoc, T. T.; Teichert, J. F. A Simple Nickel Catalyst Enabling an *E*-Selective Alkyne Semihydrogenation. *Chem.—Eur. J.* **2020**, *26*, 1597.

(18) Murugesan, D. K.; Bheeter, C. B.; Linnebank, P. R.; Spannenberg, A.; Reek, J. N.; Jagadeesh, R. V.; Beller, M. Nickel-Catalyzed Stereodivergent Synthesis of *E*- and *Z*-Alkenes by Hydrogenation of Alkynes. *ChemSusChem* **2019**, *12*, 3363.

(19) Liu, Y.; Liu, X.; Feng, Q.; He, D.; Zhang, L.; Lian, C.; Shen, R.; Zhao, G.; Ji, Y.; Wang, D. Intermetallic Ni_xM_y (M= Ga and Sn) Nanocrystals: A Non-precious Metal Catalyst for Semi-Hydrogenation of Alkynes. *Adv. Mater.* **2016**, *28*, 4747−4754.

(20) Pape, F.; Thiel, N. O.; Teichert, J. F. Z-Selective Copper(I)-Catalyzed Alkyne Semihydrogenation with Tethered Cu−Alkoxide Complexes. *Chem.—Eur. J.* **2015**, *21*, 15934−15938.

(21) Alig, L.; Fritz, M.; Schneider, S. First-Row Transition Metal (De) Hydrogenation Catalysis Based On Functional Pincer Ligands. *Chem. Rev.* **2019**, *119*, 2681−2751.

(22) Bullock, R. M. *Catalysis Without Precious Metals*; John Wiley & Sons: 2011.

(23) Haber, J. *Studies in Inorganic Chemistry*; Elsevier: 1994; Vol. *19*.

(24) Zhang, Y.; Hanna, B. S.; Dineen, A.; Williard, P. G.; Bernskoetter, W. H. Functionalization of Carbon Dioxide with Ethylene at Molybdenum Hydride Complexes. *Organometallics* **2013**, *32*, 3969−3979.

(25) Zhang, Y.; Williard, P. G.; Bernskoetter, W. H. Synthesis and Characterization of Pincer-Molybdenum Precatalysts for CO_2 Hydrogenation. *Organometallics* **2016**, *35*, 860−865.

(26) Silantyev, G. A.; Förster, M.; Schluschaß, B.; Abbenseth, J.; Würtele, C.; Volkmann, C.; Holthausen, M. C.; Schneider, S. Dinitrogen Splitting Coupled to Protonation. *Angew. Chem., Int. Ed.* **2017**, *56*, 5872−5876.

(27) MacLeod, K. C.; Holland, P. L. Recent Developments in the Homogeneous Reduction of Dinitrogen by Molybdenum and Iron. *Nat. Chem.* **2013**, *5*, 559−565.

(28) McSkimming, A.; Suess, D. L. Dinitrogen Binding and Activation at a Molybdenum−Iron−Sulfur Cluster. *Nat. Chem.* **2021**, *13*, 666−670.

(29) Arashiba, K.; Miyake, Y.; Nishibayashi, Y. A molybdenum complex bearing PNP-type pincer ligands leads to the catalytic reduction of dinitrogen into ammonia. *Nat. Chem.* **2011**, *3*, 120−125.

(30) Arashiba, K.; Kinoshita, E.; Kuriyama, S.; Eizawa, A.; Nakajima, K.; Tanaka, H.; Yoshizawa, K.; Nishibayashi, Y. Catalytic Reduction of Dinitrogen to Ammonia by Use of Molybdenum−Nitride Complexes Bearing a Tridentate Triphosphine as Catalysts. *J. Am. Chem. Soc.* **2015**, *137*, 5666−5669.

(31) Liao, Q.; Saffon-Merceron, N.; Mézailles, N. Catalytic Dinitrogen Reduction at the Molybdenum Center Promoted by a Bulky Tetradentate Phosphine Ligand. *Angew. Chem., Int. Ed.* **2014**, *53*, 14206−14210.

(32) Chakraborty, S.; Berke, H. Homogeneous Hydrogenation of Nitriles Catalyzed by Molybdenum and Tungsten Amides. *ACS Catal.* **2014**, *4*, 2191−2194.

(33) Chakraborty, S.; Blacque, O.; Fox, T.; Berke, H. Hydrogenation of Imines Catalyzed by Trisphosphine-Substituted Molybdenum and Tungsten Nitrosyl Hydrides and Co-Catalytic Acid. *Chem.—Asian J.* **2014**, *9*, 2896−2907.

(34) Chakraborty, S.; Blacque, O.; Fox, T.; Berke, H. Highly Active, Low-Valence Molybdenum-and Tungsten-Amide Catalysts for Bifunctional Imine-Hydrogenation Reactions. *Chem.—Asian J.* **2014**, *9*, 328−337.

https://doi.org/10.1021/acs.organomet.1c00709
Organometallics 2022, 41, 1797−1805

(35) Chakraborty, S.; Blacque, O.; Berke, H. Ligand Assisted Carbon Dioxide Activation and Hydrogenation Using Molybdenum and Tungsten Amides. *Dalton Trans.* **2015**, *44*, 6560−6570.
(36) Chakraborty, S.; Blacque, O.; Fox, T.; Berke, H. Trisphosphine-Chelate-Substituted Molybdenum and Tungsten Nitrosyl Hydrides as Highly Active Catalysts for Olefin Hydrogenations. *Chem.—Eur. J.* **2014**, *20*, 12641−12654.
(37) Joannou, M. V.; Bezdek, M. J.; Chirik, P. J. Pyridine(diimine) Molybdenum-Catalyzed Hydrogenation of Arenes and Hindered Olefins: Insights into Precatalyst Activation and Deactivation Pathways. *ACS Catal.* **2018**, *8*, 5276−5285.
(38) Vielhaber, T.; Faust, K.; Topf, C. Group 6 Metal Carbonyl Complexes Supported by a Bidentate PN Ligand: Syntheses, Characterization, and Catalytic Hydrogenation Activity. *Organometallics* **2020**, *39*, 4535−4543.
(39) Leischner, T.; Spannenberg, A.; Junge, K.; Beller, M. Molecular Defined Molybdenum−Pincer Complexes and Their Application in Catalytic Hydrogenations. *Organometallics* **2018**, *37*, 4402−4408.
(40) Leischner, T.; Suarez, L. A.; Spannenberg, A.; Junge, K.; Nova, A.; Beller, M. Highly Selective Hydrogenation of Amides Catalysed by a Molybdenum Pincer Complex: Scope and Mechanism. *Chem. Sci.* **2019**, *10*, 10566−10576.
(41) Leischner, T.; Spannenberg, A.; Junge, K.; Beller, M. Synthesis of Molybdenum Pincer Complexes and Their Application in the Catalytic Hydrogenation of Nitriles. *ChemCatChem.* **2020**, *12*, 4543−4549.
(42) (a) Alberico, E.; Beller, M.; Spannenberg, A.; Baumann, W.; Seifert, J.; Sang, R.; Junge, K.; Junge, H.; Leischner, T.; Kammer, A. HCOOH Disproportionation to MeOH promoted by Molybdenum PNP Complexes. *Chem. Sci.* **2021**, *12*, 13101−13119. (b) Alberico, E.; Beller, M.; Spannenberg, A.; Baumann, W.; Seifert, J.; Sang, R.; Junge, K.; Junge, H.; Leischner, T.; Kammer, A. Correction for "HCOOH Disproportionation to MeOH promoted by Molybdenum PNP Complexes. *Chem. Sci.* **2021**, *12*, 15772−15774.
(43) Wang, Y.; Zhu, L.; Shao, Z.; Li, G.; Lan, Y.; Liu, Q. Unmasking the Ligand Effect in Manganese-Catalyzed Hydrogenation: Mechanistic Insight and Catalytic Application. *J. Am. Chem. Soc.* **2019**, *141*, 17337−17349.
(44) Papa, V.; Cabrero-Antonino, J. R.; Alberico, E.; Spanneberg, A.; Junge, K.; Junge, H.; Beller, M. Efficient and Selective Hydrogenation of Amides to Alcohols and Amines Using a Well-Defined Manganese−PNN Pincer Complex. *Chem. Sci.* **2017**, *8*, 3576−3585.
(45) Gottlieb, H. E.; Kotlyar, V.; Nudelman, A. NMR Chemical Shifts of Common Laboratory Solvents as Trace Impurities. *J. Org. Chem.* **1997**, *62*, 7512−7515.
(46) Fulmer, G. R.; Miller, A. J.; Sherden, N. H.; Gottlieb, H. E.; Nudelman, A.; Stoltz, B. M.; Bercaw, J. E.; Goldberg, K. I. NMR Chemical Shifts of Trace Impurities: Common Laboratory Solvents, Organics, and Gases in Deuterated Solvents Relevant to the Organometallic Chemist. *Organometallics* **2010**, *29*, 2176−2179.
(47) Elangovan, S.; Garbe, M.; Jiao, H.; Spannenberg, A.; Junge, K.; Beller, M. Hydrogenation of Esters to Alcohols Catalyzed by Defined Manganese Pincer Complexes. *Angew. Chem., Int. Ed.* **2016**, *128*, 15590−15594.
(48) Adam, R.; Alberico, E.; Baumann, W.; Drexler, H. J.; Jackstell, R.; Junge, H.; Beller, M. NNP-Type Pincer Imidazolylphosphine Ruthenium Complexes: Efficient Base-Free Hydrogenation of Aromatic and Aliphatic Nitriles under Mild Conditions. *Chem.—Eur. J.* **2016**, *22*, 4991−5002.
(49) Dieck, H. T.; Friedel, H. Über π-Allyl-Komplexe des Molybdäns II. Die Bildung von π-Allyldicarbonylmolybdän-Komplexen aus Molybdän-hexacarbonyl und seinen Derivaten. *J. Organomet. Chem.* **1968**, *14*, 375−385.
(50) Friedel, H.; Renk, I. W.; Dieck, H. T. Komplexchemie von Vierzentren-π-Systemen IV. Synthese und Eigenschaften hochsubstituierter Molybdän-Carbonyl-Derivate. *J. Organomet. Chem.* **1971**, *26*, 247−259.
(51) Anderson, S.; Cook, D. J.; Hill, A. F. Metallathiirenes. 3.1 Thiocarbamoyl and Alkoxythiocarbonyl Complexes of Molybdenum(II) and Tungsten(II). *Organometallics* **2001**, *20*, 2468−2476.

https://doi.org/10.1021/acs.organomet.1c00709
Organometallics 2022, 41, 1797−1805